

**Sediment Incipience in Turbulence Generated in a Square Tank by a Vertically Oscillating Grid**

Author

Liu, C, Huhe, A, Tao, L

Published

2006

Journal Title

Journal of Coastal Research

Rights statement

© 2006 Coastal Education and Research Foundtion, Inc. (CERF). Please refer to the Journal of Coastal Research for access to the definitive, published version. This Special Issue is not available online. This is the author-manuscript version of this paper.

Downloaded from

<http://hdl.handle.net/10072/11881>

Link to published version

<http://www.cerf-jcr.org/>

Griffith Research Online

<https://research-repository.griffith.edu.au>

--	--	--	--	--	--

# Sediment Incipience in Turbulence Generated in a Square Tank by a Vertically Oscillating Grid

C. Liu<sup>†</sup>, Huhe Aode<sup>†</sup> and L. Tao<sup>‡</sup>

<sup>†</sup>Institute of Mechanics, Chinese Academy of Sciences, Beijing, 100080, P.R. China  
[carlliu1972@sina.com](mailto:carlliu1972@sina.com)  
[hhad@imech.ac.cn](mailto:hhad@imech.ac.cn)

<sup>‡</sup>School of Engineering, Griffith University, Gold Coast PMB50, Gold Coast Mail Centre, QLD9726, Australia  
[l.tao@griffith.edu.au](mailto:l.tao@griffith.edu.au)

## ABSTRACT

LIU, C.; HUHE AODE and TAO, L. T., 2004. Sediment Incipience in Turbulence Generated in a Square Tank by a Vertically Oscillating Grid.  
(Leave the number of pages blank)

The failure of hydraulic structures in many estuaries and coastal regions around the world has been attributed to sediment transport and local scour. The sediment incipience in homogenous turbulence generated by oscillating grid is studied in this paper. The turbulent flow is measured by particle tracer velocimetry (PTV) technique. The integral length scale and time scale of turbulence are obtained. The turbulent flow near the wall is measured by local optical magnification. The sediment incipience is described by static theory. The relationship of probability of sediment incipience and the turbulent kinetic energy were obtained experimentally and theoretically. The distribution of the turbulent kinetic energy near the wall is found to obey the power law and the turbulent energy is further identified as the dynamic mechanism of sediment incipience.

**ADDITIONAL INDEX WORDS:** *Sediment incipience, turbulence, oscillating grid, particle tracer velocimetry*

## INTRODUCTION

The sediment incipience is a classical problem in coastal hydrodynamics. For instance, the sediment transport in rivers, coastal and harbor areas. The incipient motion of sediment has been widely studied in the flow in the straight flume (RIJIN, 1984a, 1984b, QIAN and WANG, 1983), and traditionally treated with a critical bed shear stress or mean velocity. However, in some cases, the sediment is picked up due to turbulence under the condition of zero bed shear stress such as the vicinity of the reattachment point and the flow in a scour hole. Limited studies on the sediment incipience under the condition of zero mean velocity or shear stress have been reported (LYN, 1995). Several issues closely related to the sediment incipience in coastal hydrodynamics, such as the impact of turbulence on the sediment incipience, and the sediment incipient probability, have not been resolved.

In order to study the sediment incipience in the case of zero shear stress, a turbulence generated by a vertically oscillating grid in a square tank was adopted as flow model. This turbulent flow is a classical model for turbulent study and investigated by many researchers (THOMPSON and TURNER, 1975, HOPFINGER and TOLY, 1976, HANNOUN, 1988). However, little has been done on the turbulent characteristics near the wall and it is very important to the sediment incipience.

In this paper, the turbulent characteristic near the wall is studied. The turbulent kinetic energy near the wall was obtained and the sediment incipient probability was also measured. The relationship of the sediment incipient probability and the turbulent kinetic energy is presented.

## EXPERIMENTAL APPARATUS AND METHODS

The present experiments were carried out in a water tank of square cross-section, 254mm×254mm and 425mm deep as sketched in Figure 1. The vertical oscillating grid was made from square Perspex rods of side 10mm, and length 245mm with a mesh size of 50mm. The oscillating grid system were mounted at the mid-depth on a central spindle and oscillated vertically with frequencies  $f$  between 2-6Hz and amplitude  $S$  of 10mm-30mm. A Perspex box of square cross-section, 250×250mm, and 50mm deep that contains sediment was fixed at 130mm-200mm depth away from grids. The density of the sediment is  $\rho_s = 1160\text{kg/m}^3$ , and the diameter  $d_{50} = 0.45\text{mm}$ . The flow velocity was measured by the technique of particle tracer velocimetry (PTV). In order to measure the turbulent flow near the wall, the optical amplification technique was employed. The smallest vortex scale that can be resolved in this paper is  $6\lambda$ , where  $\lambda$  is Kolmogorov scale. The sediment incipient events, i.e. the area  $A_i$  and time  $T_i$  of a sediment incipient event, the number of sediment incipient events  $N$  occurred during certain time  $\Delta T$  and on certain bed area  $A$  is obtained by the Grey-Scale technique. The sediment incipient probability  $P_i$  is then calculated by

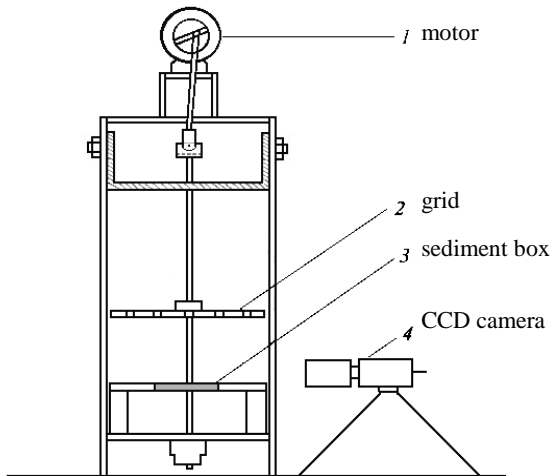


Figure 1. Sketch of the experiment.

$$P_i = \frac{\sum_{i=1}^N A_i T_i}{A \Delta T} \quad (1)$$

## RESULTS AND DISCUSSION

### PTV measurements in a homogeneous turbulence

In this section the homogenous turbulence generated by a vertically oscillating grid in a square tank in the absence of the wall will be described briefly. The instantaneous velocity field was measured by PTV technique. It is found that the flow produced by the oscillating grids has three patterns: First, near each grid bar, there is a small quasi-steady jet; Then many small jets interact and break down to produce turbulence; Finally, this turbulence decays with distance away from the grid. The root-mean-square (horizontal and vertical) turbulent velocity, Reynolds stress, integral length scale  $L$  and time scale  $\tau$  are also obtained by the method of statistical average.

In Figure 2, the horizontal and vertical root-mean-square turbulent velocity  $u', v'$  are plotted against  $Y$ , where  $Y$  is a distance away from a virtual origin coinciding with middle position of the grid. It can be seen in Figure 2 that  $u'$  and  $v'$  are almost identical and the law of the form  $u', v' \propto 1/Y$  can be used to express the experimental data when the distance from the grid is greater than  $2S$ . However, when the distance from the grid is smaller than  $2S$ , the power law of root-mean-square turbulent velocity decaying is not suitable. These results agree with Hopfinger's very well.

Figure 3 shows the variation of Reynolds stress with the distance away from the grid. It is shown in Figure 3 that Reynolds stress has a high value in the region near the grid. This

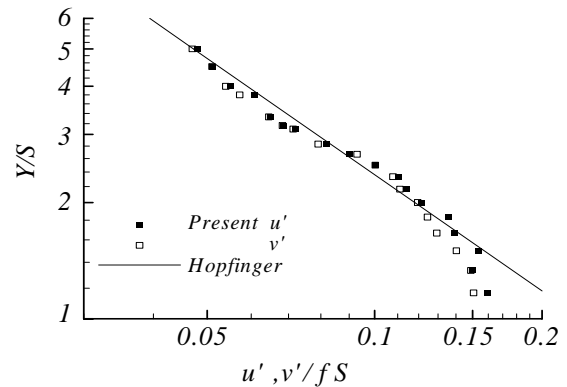


Figure 2. The variation of root-mean-square turbulent velocities with the distance away from the middle position of the grid.

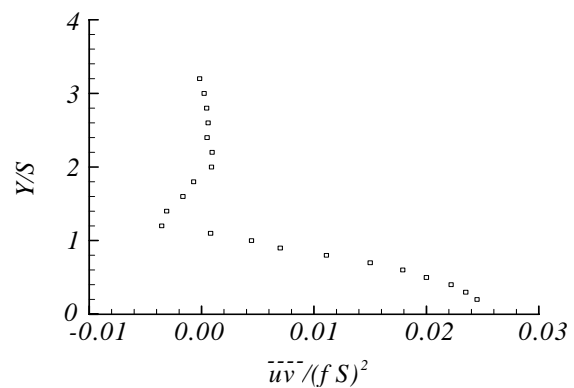


Figure 3. The variation of Reynolds stress with the distance away from the grid.

phenomenon may be explained by the jets generated under the oscillating grid. The shear layer at the fringe of the jet leads to the high Reynolds stress. Turbulence develops due to the interaction of the jets as the distance from the grid increases. Also shown in the Figure is that Reynolds stress approaches zero when the distance from the grid is greater than  $2S$ . This is due to the energy of the jets being translated to the energy of the turbulence. Therefore, in the region far from the grid, the turbulent flow generated by oscillating grid can be regarded as zero-shear stress flow.

Figure 4 shows a linear increase of the integral length scale  $L$  with the distance from the grid. Figure 5 shows that the integral time scale  $\tau$  can be represented by the function of the form  $\tau \propto Y^2$ . These results agree very well with those of THOMPSON and TURNER (1975) and HANNOUN (1988).

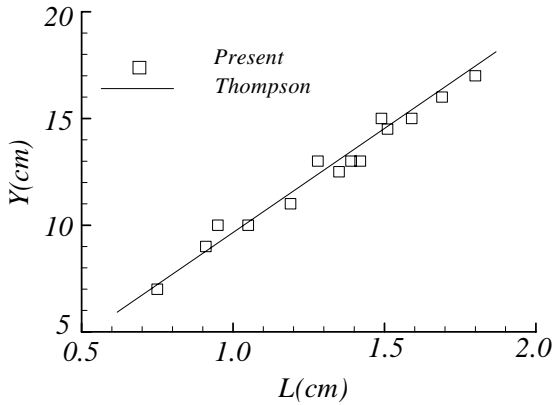


Figure 4. The variation of integral length scale with the distance away from the grid.

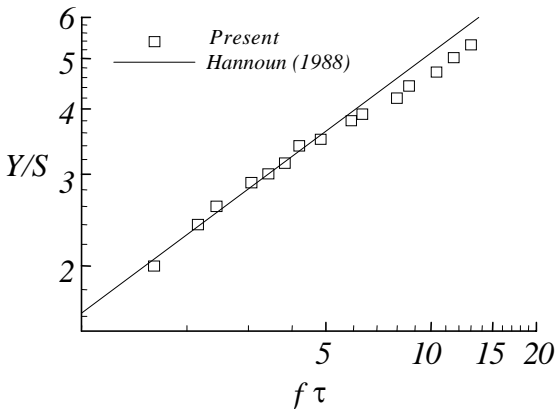


Figure 5. The variation of integral time scale with the distance away from the grid.

### Characteristics of turbulence near the wall

Since the effect of the wall on the homogenous turbulence is limited to the region of one integral length scale  $L$ , the turbulent flow filled within an integral length scale was measured by the technique of PTV in this study. The values of the root-mean-square (horizontal and vertical) turbulent velocity and the turbulent energy near the wall are then obtained.

The variation of the non-dimensional root-mean-square turbulent velocity  $u'/u'_0$ ,  $v'/v'_0$  with the non-dimensional distance away from the wall  $\zeta/L_0$  is showed in Figure 2.

Where  $L_0$  is the integral length scale of the homogenous turbulence at the location of the wall and subscript 0 refers to the quantities in homogenous turbulence in the absence of the wall. It is found that the effect of the wall is very small when  $\zeta/L_0 > 1$  and the horizontal velocity is magnified and the

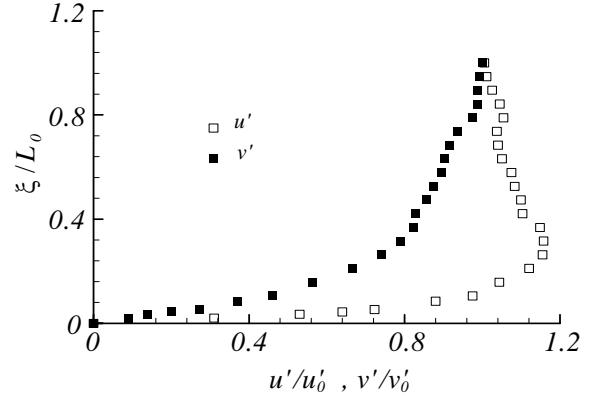


Figure 6. The variation of the non-dimensional root-mean-square turbulent velocity with the non-dimensional distance away from the wall.

vertical velocity is attenuated when  $0.3 < \zeta/L_0 < 1$  due to the deformation of the large-scale vortex. Both the horizontal and vertical velocities are attenuated due to viscous effect when  $\zeta/L_0 < 0.3$ .

The turbulent kinetic energy in the region of one integral length away from the wall is obtained. It is found that the turbulent kinetic energy near the wall is approximately equal to that of homogenous turbulence in the absence of the wall when the distance away from the wall is much larger than  $\sqrt{\nu\tau_0}$ , and decreases when the distance away from the wall is in the order of  $\sqrt{\nu\tau_0}$  due to viscous effect, where  $\nu$  is the kinematic viscosity and  $\tau_0$  is the integral time scale of the homogenous turbulence at the location of the wall. It is a clear indication that the thickness of the viscous sublayer is the same order of  $\sqrt{\nu\tau_0}$ . The turbulent flow field in the viscous sublayer was then measured in cases of different grid strokes, oscillating frequencies and the distance from the grid to the wall  $Y_w$ . The results of turbulent kinetic energy within the viscous sublayer are shown in Figure 7. It can be seen in Figure 7 that all experimental data can be expressed by the law of power:

$$\frac{\overline{k_w}}{\overline{k_0}} = A \left( \frac{\zeta}{\sqrt{\nu\tau_0}} \right)^B \quad (2)$$

where  $\overline{k_w}$ ,  $\overline{k_0}$  is turbulent kinetic energy with and without the effect of the wall respectively,  $A$  and  $B$  are constants.

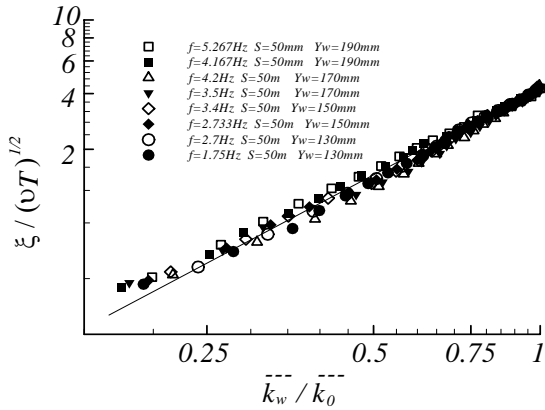


Figure 7. The variation of turbulent energy with the distance away from the wall within a viscous sublayer.

### The probability of sediment incipience

The forces acting on a sediment particle include its submerged weight, hydrodynamic fluid forces and the forces of the bed acting on it. If the hydrodynamic fluid forces are large enough to overcome the other forces, the sediment particle will be picked up by fluid. Assumed that the forces of the fluid acting on the sediment particles are dependent on the instant velocity near the wall (BELOSHAPKOVA, 1992), the probability of sediment incipience  $P_i$  is the probability of that the instant velocity near the wall  $u_w$  is greater than the sediment incipient velocity  $u_c$ :

$$P_i = P\{u_w > u_c\} \quad (3)$$

As demonstrated previously, the horizontal velocity is magnified and the vertical velocity is attenuated near the wall. The magnitude of the instant velocity near the wall can be assumed to be equal to the magnitude of horizontal velocity:

$$u_w = \sqrt{u_x^2 + u_z^2} \quad (4)$$

in which  $u_x$  and  $u_z$  are the velocity components in horizontal direction. The probability density of  $u_x$  and  $u_z$  can be assumed to satisfy the Gaussian distribution (TAVOULARIS and CORRISIN, 1981):

$$p(u_x) = \frac{1}{\sqrt{2\pi}u'} e^{-\frac{u_x^2}{2u'^2}} \quad (5)$$

$$p(u_z) = \frac{1}{\sqrt{2\pi}u'} e^{-\frac{u_z^2}{2u'^2}}$$

where the root-mean-square turbulent velocity  $u'$  can be expressed by turbulent kinetic energy:

$$u'^2 = \overline{k_w} \quad (6)$$

The probability of sediment incipience is obtained by equations (3) ~ (6):

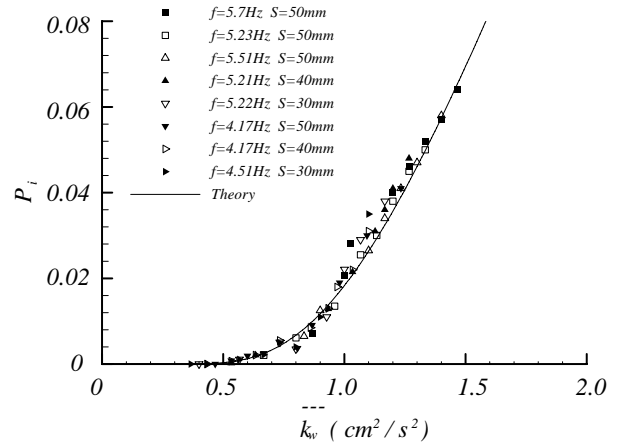


Figure 8. The relationship of the probability of sediment incipience and the turbulent kinetic energy.

$$P_i = e^{-k_c / \overline{k_w}} \quad (7)$$

where  $\overline{k_w}$  is the turbulent kinetic energy at the position of  $0.5d_{50}$  away from the wall and  $k_c$  is the critical turbulent kinetic energy of sediment incipience. It is noted that  $k_c$  is constant for certain sediment.

The probability of sediment incipience is calculated based on the turbulent kinetic energy measured in the experiment for the case of different grid strokes, oscillating frequencies and the distance from the grid to the wall. The relationship of the probability of sediment incipience and the turbulent kinetic energy obtained by experiment is presented in Figure 8. As can be seen in the figure, all experimental data can be predicted by equation (7) in the case of different flow conditions. This indicates that for the non-shear flow the sediment incipient probability is dependent only on the turbulent energy near the wall for certain sediment and the turbulent energy can be taken as the dynamic mechanism of sediment incipience. The constant number  $k_c$  can be determined according to the experimental data. The non-dimensional critical turbulent kinetic energy of sediment incipience can be defined as

$$Sh_c = \frac{\rho_w k_c}{(\rho_s - \rho_w)gd_{50}} \quad (8)$$

where,  $\rho_w$  is the density of the water,  $g$  is the gravity acceleration. Similar to Shields number,  $Sh_c$  is the critical criterion of sediment incipience in the case of non-shear flow. Due to the limitation of experiment apparatus, only one  $Sh_c$  for certain sediment is presented in this paper. The value of  $Sh_c$  for the sediment in this paper is 0.37, and its Shields number is 0.051.

## CONCLUSION

The flow velocities of the turbulence generated by oscillating grid was measured by PTV technique. The probability of sediment incipience in the case of zero shear stress flow was studied. It is found the distribution of the turbulent kinetic energy near the wall obeys the law of power and the probability of sediment incipience increases with turbulent kinetic energy by the law of exponent. The non-dimensional critical turbulent kinetic energy can be the critical criterion of sediment incipience in the case of non-shear flow.

## LITERATURE CITED

- BELOSHAPKOVA, S.G., 1992. On the causes of the onset of sediment movement. *Okeanologia*, 32, pp. 347-353.
- HANNOUN I.A., 1988. Turbulence Structure Near a Sharp Density Interface. *Journal of Fluid Mechanics*, 189, pp. 189-209
- HOPFINGER, E.J. and TOLY, J.A., 1976. Spatially decaying turbulence and its relation to mixing across density interfaces. *Journal of Fluid Mechanics*, 78, pp. 155-175
- LYN, D.A., 1995. Observation of initial sediment motion in a turbulent flow generated in a square tank by a vertically oscillating. *Water Resource Engineering, Proceedings of the First International Conference*, San Antonio, Texas, pp. 609-613.
- QIAN, N. and WANG, Z.H., 1983. *Sediment Dynamics*. Academic Press, Beijing.
- RIJIN, L.C.V., 1984a. Sediment transport, Part I: Bed Load transport. *Journal of Hydraulic Engineering*, ASCE, 110, pp. 1431-1455.
- RIJIN, L.C.V., 1984b. Sediment pick-up function. *Journal of Hydraulic Engineering*, ASCE, 110, 1494-1502.
- TAVOULARIS, S. and CORRSIN, S., 1981. Experiments in nearly homogenous turbulent shear flow with a uniform temperature gradient. *Journal of Fluid Mechanics*, 104, pp. 311-347.
- THOMPSON, S.N. and TURNER, J.S., 1975. Mixing at an Interface Due to Turbulence Generated by an Oscillating Grid. *Journal of Fluid Mechanics*, 67, pp. 349-368